

# Growth of atomically smooth cubic AlN by molecular beam epitaxy

Thorsten Schupp<sup>\*1</sup>, Georg Rossbach<sup>2</sup>, Pascal Schley<sup>2</sup>, Rüdiger Goldhahn<sup>2</sup>, Klaus Lischka<sup>1</sup> and Donat Josef As<sup>\*\*1</sup>

<sup>1</sup> Department of Physics, University of Paderborn, Warburger Str. 100, 33095 Paderborn, Germany

<sup>2</sup> Institut für Physik, Technische Universität Ilmenau, PF 100565, 98684 Ilmenau, Germany

Received 19 June 2009, revised 8 August 2009, accepted 26 September 2009

Published online 9 December 2009

PACS 61.05.jh, 68.37.Ps, 68.55.ag, 78.66.Fd, 81.05.Ea, 81.15.Hi

\* Corresponding author: e-mail [tshupp@mail.uni-paderborn.de](mailto:tshupp@mail.uni-paderborn.de), Phone: +49 5251 60 5831, Fax: +49 5251 60 5843

\*\* e-mail [d.as@uni-paderborn.de](mailto:d.as@uni-paderborn.de), Phone: +49 5251 60 5838, Fax: +49 5251 60 5843

In this work we present the growth of atomically flat c-AlN layers (surface roughness 0.3 nm RMS) by plasma assisted molecular beam epitaxy (PAMBE) on 3C-SiC. We develop a model for Al surface kinetics that correlates with RHEED intensity vs. time measurements. We show RHEED patterns and atomic force microscopy (AFM) scans emphasizing the quality of the layers.

Ellipsometry yields the dielectric function of c-AlN around the adsorption edge. The direct gap is obtained with 5.93 eV at room temperature, while the indirect one is below 5.3 eV (onset of adsorption)

© 2010 WILEY-VCH Verlag GmbH & Co. KGaA, Weinheim

**1 Introduction** The wide-bandgap semiconductors AlN, GaN and their alloys have a hardness comparable to sapphire, a high chemical stability and a large thermal conductivity. In contrast to the natural hexagonal phase the metastable cubic phase of AlN (c-AlN) and GaN (c-GaN) has no polarization electrical fields in growth direction [1]. This set of properties make them candidates for efficient deep UV photonic devices and high power electronic devices.

The surface roughness is of great importance for nanoscale devices as high roughness can lead to shortcuts in electronic devices and broadening of confined electronic states of low dimensional structures. In the past cubic AlN has shown considerable roughness and a tendency to form hexagonal inclusions [2, 3].

In this contribution we report on the PAMBE growth of atomically flat c-AlN layers with a surface roughness around 0.3 nm RMS. A model for the Al surface kinetics is developed that links the Al surface coverage with the intensity of reflections in the RHEED pattern. Furthermore RHEED patterns and atomic force microscopy (AFM) scans are shown that validate the quality of the c-AlN layers. Last but not least we present the dielectric function of c-AlN around the bandgap obtained by ellipsometry including the direct and indirect bandgap.

**2 Experimental** Cubic AlN layers were grown pseudomorphically strained on freestanding 3C-SiC (001) substrates by PAMBE in a Riber 32 growth chamber [4]. Ga and Al were evaporated from Riber effusion cells, N was generated by an Oxford Instruments RF plasma source. At first the substrate was cleaned in an ultrasonic bath by acetone, propanol and buffer oxide etching (BOE). Deoxidation was done in the MBE chamber by repeatedly depositing and desorbing Al layers (Al flashes) at 900 °C substrate temperature and an Al flux of  $3 \times 10^{14} \text{ cm}^{-2} \text{ s}^{-1}$  [5]. The growth of the c-AlN layer started with the deposition of one monolayer (ML) of Al on the surface at the growth substrate temperature of 730 °C. The growth parameters used are, Al flux of  $2 \times 10^{14} \text{ cm}^{-2} \text{ s}^{-1}$  and N<sub>2</sub> flux of 1.5 sccm at a plasma setting of 300 W respectively. In situ growth monitoring is done by reflection high electron energy diffraction (RHEED) [6]. The growth rate of 150 nm/h was determined by RHEED specular spot intensity oscillations (RHEED oscillations). The growth was stopped at 300 nm to prevent roughness transitions which are related to the relaxation of the strained c-AlN layer on the 3C-SiC substrate.

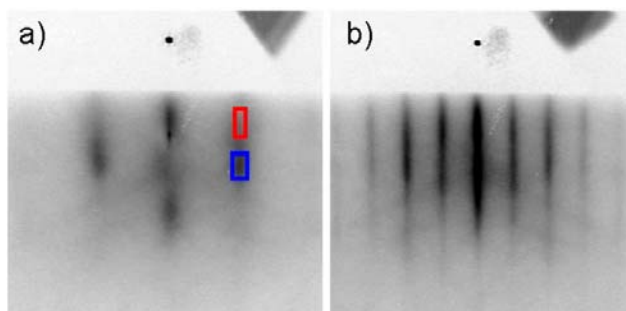


**Figure 1** RHEED images observed during the cleaning process of 3C-SiC. (a) [-110] azimuth of the 3C-SiC substrate before Al flashes, (b) [-110] azimuth of the 3C-SiC substrate after Al flashes.

### 3 Results and discussion

**3.1 Deoxidation** Figure 1(a) shows the RHEED pattern of the 3C-SiC (001) surface in [-110] azimuth. The reflections of the cubic lattice are blurred by surface oxides, the elliptical shape indicates an electron transmission component originating from three dimensional islands on the surface [7]. Figure 2 shows the intensity over time of two spots in the substrate RHEED pattern during the repeated deposition and desorption of Al layers. The blue graph shows the RHEED intensity associated with the 3D islands on the surface, whereas the red graph shows the RHEED intensity associated with the 2D part of the surface. The intensity of the blue graph decreases with each cycle, indicating a reduction of the 3D oxide islands. The intensity of the red graph and the amplitude of both graphs increases, indicating a reduction in surface roughness and an increase of surface sensitivity.

At the end of the cleaning process the RHEED pattern of

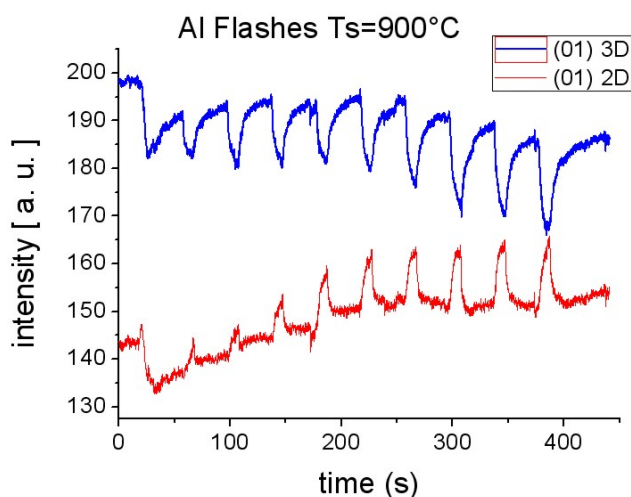


**Figure 2** Intensity over time measurement of two spots in the RHEED pattern of the 3C-SiC surface during the repeated deposition and desorption of Al.

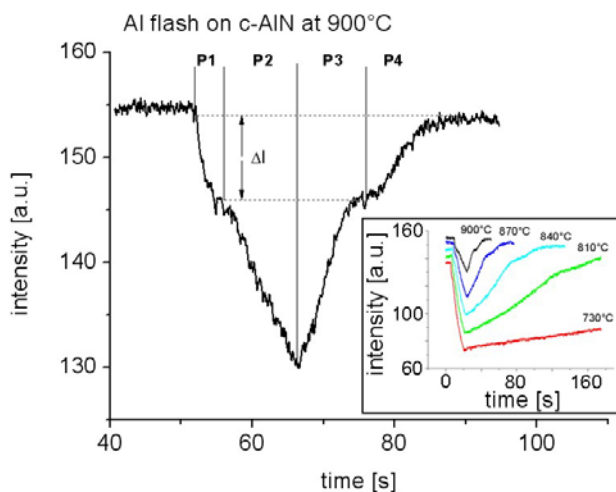


**Figure 3** Intensity over time measurement of the [01] RHEED reflection of the c-AlN surface during the deposition and desorption of Al. The inserted window shows the intensity graphs for various substrate temperatures.

the 3C-SiC surface in Fig. 1(b) shows long thin streaks indicating a two dimensional oxide free surface with a (2x4) reconstruction.

**3.2 Al surface kinetics** Cubic AlN is a metastable form of AlN, therefore exposing a c-AlN surface to nitrogen leads to the formation of hexagonal clusters. Hexagonal condensation can be prevented by growing under Al rich conditions with one monolayer Al surface coverage. To maintain one ML Al coverage a model linking the Al surface coverage and RHEED intensity has been developed. It is based on a model used for Ga on c-GaN introduced by Schörmann et al. [8]. The key element is a difference in RHEED intensity between a c-AlN surface and an Al surface. Figure 3 shows the intensity over time of the RHEED (01) spot of a c-AlN layer during the deposition and desorption of Al for various substrate temperatures. All graphs show a distinct kink at  $\Delta I$  below their maximum intensity on the adsorption and desorption side. The intensity change between the maximum intensity and that kink is linked to the Al surface coverage on c-AlN. According to the model an Al flash consists of 4 phases as shown in the Fig. 3. Phase 1 is the adsorption of the first monolayer of Al on the c-AlN surface. It begins at zero Al coverage and ends at one monolayer. Phase 2 is the formation of Al droplets on the surface leading to further intensity decrease. Phase 3 is the desorption of the Al droplets. During this phase there is also desorption from the Al monolayer, however the droplets act as reservoirs of Al which feed the monolayer and stabilize the one monolayer coverage. Phase 4 is the desorption of the Al monolayer.

**3.3 Growth of cubic AlN** After the deposition of one monolayer of Al on the surface and an interruption of 10 seconds, the growth begins by simultaneously opening the Al and N shutter.

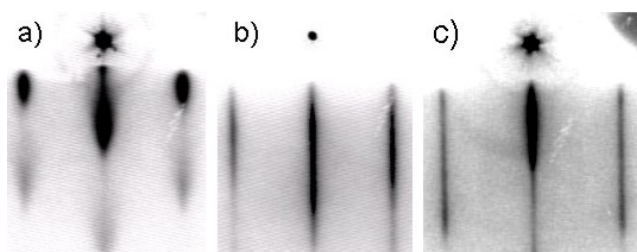


**Figure 4** RHEED images of the c-AlN surface during the initial growth process. (a) after the growth of 4 ML, (b) after the growth of 30 ML, (c) after the growth of 685 ML

Comparing the RHEED pattern of the substrate in Fig. 1(b) with the RHEED pattern after the deposition of 4 ML of c-AlN in Fig. 4(a) indicates a transition from a 2D to 3D surface. This can be seen by the transformation of long streaks into spotty reflections originating from an electron transmission component through islands on the surface. After 20 monolayers a roughness transition is observed, transforming the surface back to an atomically smooth 2D state. This can be seen in the RHEED pattern of the c-AlN surface in Fig. 4(b) by long thin streaks and the lack of spotty reflections. After the completion of the initial growth the c-AlN layers were grown in cycles of 20 atomic layers, with growth interruptions of 30 seconds. The c-AlN thickness was controlled by RHEED oscillations, where every oscillation indicates the growth of one atomic layer. The growth rate was determined to be 0.2 ML/s from RHEED oscillations as shown in Fig. 5. After the growth of 150 nm (685 ML) c-AlN the RHEED pattern as seen in Fig. 4(c) still indicates a smooth 2D surface. All azimuths show RHEED patterns of the cubic lattice, hexagonal reflections are absent. These findings are supported by x-ray measurements, not presented here, which show the reflection from cubic

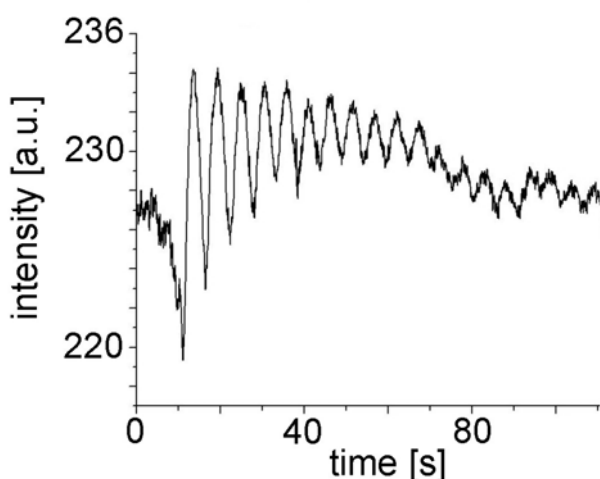


**Figure 5** RHEED specular spot intensity over time measurement. Each oscillation equals the growth of one atomic layer of c-AlN.

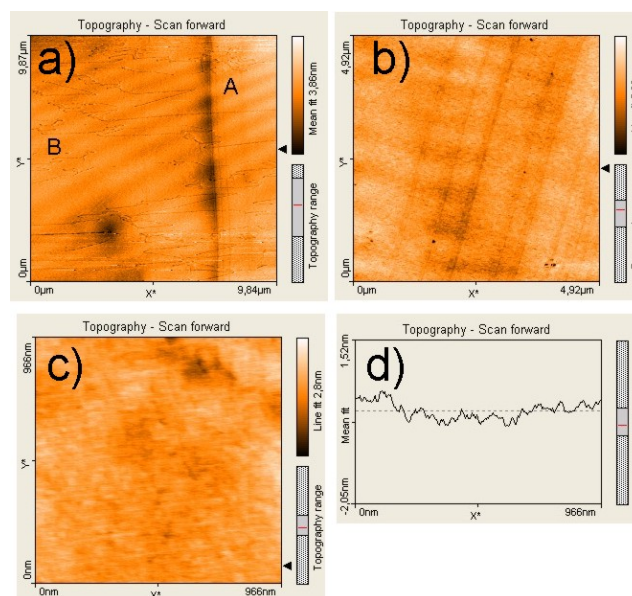


**Figure 6** AFM images: (a)  $10 \times 10 \mu\text{m}^2$  area of the 3C-SiC substrate, (b)  $5 \times 5 \mu\text{m}^2$  area of the 150nm thick c-AlN layer, (c)  $1 \times 1 \mu\text{m}^2$  area of the c-AlN layer with a roughness of 0.2 nm RMS, (d) line scan of Fig. 6(c).

AlN close to the 3C-SiC substrate. Using this method c-AlN layers up to 300 nm thickness have been grown.

**3.4 Atomic force microscopy** The AFM image in Fig. 6(a) shows a  $10 \times 10 \mu\text{m}^2$  area of the 3C-SiC substrate surface. Around letter A parallel lines originating from anti boundary defects can be identified. Secondly line defects originating from surface oxides can be seen around letter B. The third effect is a wave pattern over the entire surface, which is an AFM measurement artifact known from smooth surfaces [9]. The RMS surface roughness including boundary defects is 1 nm and 0.5 nm without the defects. Fig. 6(b) shows a  $5 \times 5 \mu\text{m}^2$  area of the atomically smooth c-AlN surface with parallel lines originating from anti boundary defects. Including the anti boundary defects the surface roughness is 0.6 nm RMS. Furthermore a wave pattern can be seen which originates from the same measurement artifact seen on the substrate. Fig. 6(c) shows an AFM image of an  $1 \times 1 \mu\text{m}^2$  area with a roughness of 0.2 nm RMS. The line scan of Fig. 6(d) depicts a peak-to-valley height of only 1 lattice constant over a lateral extension of  $\sim 2000$  lattice constants.

**3.5 Ellipsometry** Ellipsometry measurements were performed under different angles of incidence. The dielectric function (DF) is obtained by a multi-layer fitting procedure similar to the approach presented in Ref. [10]. No assumption was made concerning the shape of the DF, i.e. the real ( $\epsilon_1$ ) and imaginary part ( $\epsilon_2$ ) of the DF was fitted for every photon energy. Figures 7 and 8 show a comparison of the real and imaginary part, respectively, for c-AlN with the ordinary data of hexagonal AlN from Ref. [11]. As can be seen in Fig. 8, the  $\epsilon_2$  function of c-AlN shows a clear shift to lower energy compared to the hexagonal reference

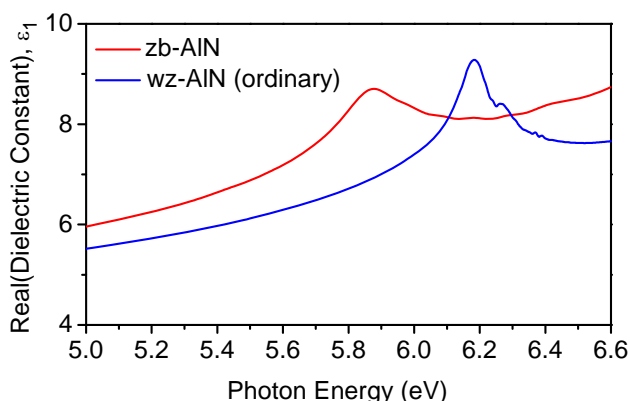


**Figure 7** Comparison of the real part of the dielectric function of cubic (red) and hexagonal (blue) AlN measured by ellipsometry.

layer. The sharp onset at 5.88 eV defines the direct excitonic band gap. Adopting the exciton binding energy of 50 meV for the hexagonal counterpart [12], we determine the direct band gap at the  $\Gamma$  point of the Brillouin zone with 5.93 eV. This result is in excellent agreement to the calculated quasi-particle band gap of 5.86 eV if the lattice polarizability is taken into account [13]. For comparison, previous studies [14] of mixed phase AlN yielded for the zinc-blende compound 5.74 eV.

The pronounced absorption tail below 5.88 eV in Fig. 8 is attributed to phonon-assisted indirect absorption. The imaginary part differs appreciably from zero only above 5.3 eV, i.e. this energy defines the upper limit of the indirect band gap. A slightly lower value might be possible as well, but ellipsometry is not sensitive enough in the case of low absorption. For comparison, the theoretical calculation presented in Refs. [13] and [15] yielded for the indirect gap of c-AlN 4.74 and 5.1 eV, respectively.

**4 Conclusion** We have grown atomically smooth c-AlN layers on 3C-SiC substrates by PAMBE. The kinetic model for the Al surface coverage was verified for various substrate temperatures enabling the growth under one monolayer of excess Al. RHEED patterns and AFM scans verified a smooth surface. However anti boundary defects originating from the substrate still show up on the c-AlN surface.

Finally we measured the dielectric function of c-AlN near the bandgap and determined a direct band gap at 5.93 eV and an indirect gap below 5.3 eV.

**Acknowledgement** We like to thank the German Research Foundation (DFG) for the project funding and the DFG graduate program “Micro- and Nanostructures in Optoelectronics and Photonics” for the scholarship.

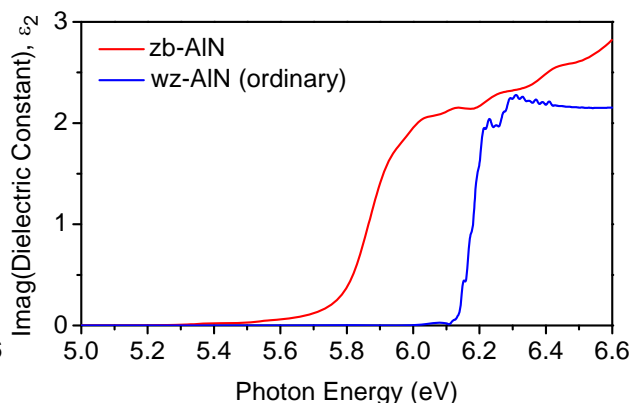


**Figure 8** Comparison of the imaginary part of the dielectric function of cubic (red) and hexagonal (blue) AlN measured by ellipsometry.

## References

- [1] J. A. Majewski, G. Zander, and P. Vogl, *Phys. Status Solidi A* **179**, 285 (2000).
- [2] B. Daudin and F. Widmann, *J. Cryst. Growth* **182**, 1 (1997).
- [3] V. Lebedev, V. Cimalla, U. Kaiser, Ch. Foerster, J. Pezoldt, J. Biskupek, and O. Ambacher, *J. Appl. Phys.* **97**, 114306 (2005).
- [4] M. P. Thompson, G. W. Auner, and A. R. Drews, *J. Electron. Mater.* **28**(10), 17 (1999).
- [5] K. H. Ploog, O. Brandt, R. Muralidharan, A. Thamm, and P. Waltereit, *J. Vac. Sci. Technol. B* **18**, 2290 (2000).
- [6] S. D. Burnham and W. A. Doolittle, *J. Vac. Sci. Technol. B* **24**, 2104 (2006).
- [7] W. Braun, *Applied RHEED*, Springer Tracts in Modern Physics, Vol. 154 (Springer, Berlin, 1999).
- [8] J. Schörmann, S. Potthast, D. J. As, and K. Lischka, *Appl. Phys. Lett.* **90**, 041918 (2007).
- [9] A. Mendez-Vilas, M. L. Gonzalez-Martín, L. Labajos-Broncano, and M. J. Nuevo, *Appl. Surf. Sci.* **238**, 42 (2004).
- [10] R. Goldhahn, S. Shokhovets, J. Scheiner, G. Gobsch, T. S. Cheng, C. T. Foxon, U. Kaiser, G. D. Kipshidze, and W. Richter, *Phys. Status Solidi A* **177**, 107 (2000).
- [11] R. Goldhahn, C. Buchheim, P. Schley, A.T. Winzer, H. Wenzel, in: *Nitride Semiconductor Devices: Principles and Simulation*, ed. by J. Piprek (Wiley VCH, Weinheim, 2007), p. 95.
- [12] T. Onuma, T. Shibata, K. Kosaka, K. Asai, S. Sumiya, M. Tanaka, T. Sota, A. Uedono, and S.F. Chichibu, *J. Appl. Phys.* **105**, 023529 (2009).
- [13] F. Bechstedt, K. Seino, P. H. Hahn, and W. G. Schmidt, *Phys. Rev B* **72**, 245114 (2005).
- [14] V. Cimalla, V. Lebedev, U. Kaiser, R. Goldhahn, C. Foerster, J. Pezoldt, and O. Ambacher, *Phys. Status Solidi C* **2**, 2199 (2005).
- [15] W. R. L. Lambrecht and B. Segall, *Phys. Rev. B* **43**, 7070 (1991).